

# Facies Modeling Accounting for the Precision and Scale of Seismic Data: Application to Albacora Field

G. Schwedersky-Neto, Marcella Maria de Melo Cortez, and Marcos Fetter Lopes  
Petrobras CENPES Research Center

C. V. Deutsch,  
Department of Civil & Environmental Engineering, University of Alberta

## Abstract

*Seismic impedance provides information on the relative proportion of different facies types. It is important to integrate such seismic data in the construction of detailed 3-D facies models, which are used for reservoir management. Two critical challenges faced in the integration of seismic impedance data: (1) the seismic data is at a larger scale than the well data / geological modeling cells, and (2) the seismic data provides soft (imprecise) information on the facies proportions within that large volume.*

*A novel block cokriging approach was developed and implemented. This method was adapted for use in sequential indicator simulation to explicitly account for the large scale soft seismic data. Conventional sequential indicator simulation and a popular alternative, SIS with Bayesian updating, were considered for comparison purposes.*

*The key challenge in applying stochastic simulation with block cokriging is the construction of a licit model of coregionalization between the “hard” well data and the “soft” seismic data. A hybrid procedure is presented that can be applied in the common case of limited well data.*

*The Albacora field offshore Brazil consists of deep water turbidite sands, shales, and cemented sands. Good quality seismic data and significant variations in facies proportions make this an excellent example to illustrate the benefit of integrating seismic data in high resolution 3-D facies modeling.*

KEYWORDS: geostatistical simulation, stochastic modeling, reservoir characterization, Bayesian updating, block cokriging

## Introduction

One goal of reservoir modeling teams is to build high resolution predictive reservoir models of facies, porosity, and permeability that, by construction, honor all available reservoir data. These numerical models provide reliable predictions of future reservoir performance at all stages of the reservoir life cycle. The unavoidable uncertainty in reservoir performance forecasting will be measured and minimized by such reliable numerical reservoir models.

The available data includes, but is not limited to, conceptual geological models, seismic data, core data, well log data, DST/RFT data, well test data, and historical production data. Each source of data carries information, at different scales and with varying levels of precision, related to the true distribution of petrophysical and fluid properties in the reservoir. Integrating all available data by construction in numerical geological models will make it possible for reservoir management teams to quickly consider numerous scenarios to optimize each reservoir management plan.

Observations and interpretations related to seismic data are particularly difficult to build into predictive reservoir models. This paper addresses this challenging aspect of data integration. Seismic data is important because it provides information in the vast interwell region; most other data provides information only within small localized volumes. The challenge is to build high resolution models that account for the large scale imprecise seismic data [3, 6, 8, 10].

Seismic-derived acoustic impedance data provides information on facies types and porosity. The emphasis of this paper is modeling facies types; the facies types are, in general, more important since they constrain the allowable range of porosity, permeability, and relative permeability. There are two different approaches to facies modeling (1) cell-based facies modeling where the spatial distribution of the facies types is statistically constrained with  $n$ -point statistics such as variograms and transition probabilities, and (2) object-based facies modeling where the spatial distribution of facies types is created with geologically realistic objects embedded within a matrix facies type. The choice of the most appropriate method depends on the depositional environment, the relative proportions of the different facies types, and the presence of diagenetic overprint.

Both approaches have their place; however, a cell-based approach is considered most appropriate for the Albacora reservoir, which was the focus of the case study. The main reason for this choice is the diagenetic cements, which defy simple object parameterization.

There are a number of different cell-based facies modeling techniques. Indicator simulation provides great flexibility, particularly for the integration of seismic data, and was used in this study. A common alternative cell-based approach is based on truncating continuous Gaussian fields [14]. This approach was not used because of the implicit nesting of the variables and the inflexibility or only one variogram. It is worth noting, however, that the “variogram downscaling” procedures developed below could be applied for truncated Gaussian simulation.

At the heart of indicator simulation is the use of kriging (spatial regression) to determine the conditional probability of each facies type. In presence of seismic data the kriging equations must be modified to *weight* the seismic data, a procedure called cokriging. Such cokriging requires a model for the spatial correlation of the facies types, the seismic data, and the cross correlation between facies types and seismic data. Inference of these models of spatial correlation is the critical problem. In addition to the mathematical constraints on such “models of coregionalization,” a confounding factor is that the seismic data is at a significantly larger scale than the well-derived indicator data. The requirement is a small scale model of coregionalization; otherwise, the cross correlation depends not only on the distance  $\mathbf{h}$  between the seismic and well data but on the relative position of the well data within the larger seismic data volume. One procedure for inference of the required model of coregionalization will be developed below [5].

The conventional sequential indicator simulation (SIS) procedure is modified to perform cokriging with large scale seismic data and small scale well data. This modified procedure explicitly accounts for the scale and precision of the seismic data. An alternative to this somewhat complex procedure is the “Bayesian updating” approach [8], which requires only the correlation (variogram) of the well data. This simpler procedure will also be considered in the case study.

The Albacora reservoir is an offshore Brazilian reservoir consisting of deepwater turbidite sands and shale. The four facies of interest are (1) clean turbidite sandstone with a minor fraction of concretions, (2) sandstone with a significant proportion of concretions, (3) sandstone with significant concretions mixed with shale, and (4) clearly non-reservoir facies consisting of shale and entirely cemented sandstone. The spatial distribution of these facies types has an overwhelming effect on fluid flow. A reservoir characterization study was undertaken to model the facies distribution. Good quality 3-D seismic data are available over the study area; the inverted impedance values are sensitive to the amount of reservoir / non-reservoir, thus is importance to include in the reservoir characterization study. The final facies models will be used for reservoir management decision making. The focus of this paper is on methods to construct facies models consistent with the well and seismic data.

## Methodology

There are  $k = 1, \dots, K$  facies types with overall average proportions of  $p_k, k = 1, \dots, K$  where  $\sum_{k=1}^K p_k = 1$ . Local well data at location  $\mathbf{u}$  are represented as a series of  $K$  indicator data defined as:

$$i(\mathbf{u}; k) = \begin{cases} 1, & \text{if facies } k \text{ prevails at location } \mathbf{u} \\ 0, & \text{otherwise} \end{cases} \quad k = 1, \dots, K \quad (1)$$

The expected values (averages) of the indicator data correspond to the global proportions  $p_k, k = 1, \dots, K$ .

The notation  $p(\mathbf{u}_\beta; k), k = 1, \dots, K$  will be used for the seismic-derived probability of facies  $k$  at block location  $\mathbf{u}_\beta$ . The modeling scale (associated to the hard well data scale) will be denoted with a  $v$  and the seismic scale will be denoted with a  $V$ . The notation  $|v|$  or  $|V|$  refers to the measure or dimension of the well and seismic data, respectively. This measure depends on direction. For example, the seismic data  $V$  is larger than the well data  $v$  in the vertical direction whereas it may coincide, or even be smaller than, the modeling cell size  $v$  in the horizontal direction.

## Sequential Indicator Simulation

The sequential indicator simulation (SIS) approach provides flexibility to integrate soft data and unique patterns of spatial correlation. An object-based approach would be difficult to apply given the lack of clear object geometries; the shales and diagenetic cements do not follow any obvious object parameterization. The SIS methodology:

1. Loop over all cells in the 3-D model in random order.
2. At each cell location:

- (a) Find nearby data: (1) well data, (2) cells that have already been informed earlier in the path, and (3) seismic data
- (b) Estimate the probability of each facies,  $k = 1, \dots, K$  (where  $K=4$  in our case) by kriging:

$$i^*(\mathbf{u}; k) = \sum_{\alpha=1}^{n_w} \lambda_{\alpha} \cdot i(\mathbf{u}_{\alpha}; k) + \sum_{\beta=1}^{n_s} \lambda'_{\beta} \cdot p(\mathbf{u}_{\beta}; k) \quad (2)$$

where  $i^*(\mathbf{u}; k), k = 1, \dots, K$  are the probabilities of facies  $k = 1, \dots, K$  to be present at location  $\mathbf{u}$ ,  $n_w$  is the number of nearby well data and previously informed cells,  $\lambda_{\alpha}, \alpha = 1, \dots, n_w$  are the weights they receive,  $i(\mathbf{u}_{\alpha}; k)$  is the probability that location  $\mathbf{u}_{\alpha}$  is in facies  $k$  (0 or 1 for these hard data),  $n_s$  is the number of nearby seismic data,  $\lambda'_{\beta}, \beta = 1, \dots, n_s$  are the weights they receive, and  $p(\mathbf{u}_{\beta}; k)$  is the probability that location  $\mathbf{u}_{\beta}$  is in facies  $k$  (between 0 to 1 depending on the acoustic impedance and the calibration with well data).

A common assumption is to take the single collocated seismic value and build a model of coregionalization that depends solely on the collocated correlation coefficient [2, 3, 15]. A number of studies have considered the impact of this assumption [6].

- (c) Assemble the estimated probabilities into a cumulative distribution. The ordering does not matter as long as the random number (next step) is not correlated with the ordering.
- (d) Draw a random number between 0 and 1 and read the corresponding facies code  $k'$  from cumulative distribution.
- (e) Assign the facies code  $k'$  to the location  $\mathbf{u}$ .

3. Return to 2 until every cell in the model has been assigned a facies code

4. Repeat with different random number seeds for multiple equally probably realizations.

This procedure is classical [1]. The key step for our purposes is how to establish the “correct” weights to give to the well data and the seismic data. There are three variants of SIS that we will consider (1) well data alone, (2) the Bayesian updating approach for simply integrating seismic data, and (3) a block cokriging approach for rigorous integration. The following steps are required to implement SIS.

## Seismic-Derived Probabilities

The seismic attribute(s) or acoustic impedance (AI) must be calibrated with the facies proportions. We should note that cokriging does not require this calibration; the original AI units could be retained and the calibration could enter through the cross variogram between the hard “i” data and soft “AI” data. Notwithstanding the flexibility of cokriging to handle untransformed AI units, we prefer the calibrated  $p(\mathbf{u}; k)$  values for a number of reasons (1) the cross variogram may be poorly informed with limited well data, and (2) the proportion / probability data are easier to interpret; they are in units we understand. There are alternative approaches to seismic calibration including [11].

<i>ai</i> -class	$p(\mathbf{u}_\beta; k = 1, ai)$	$p(\mathbf{u}_\beta; k = 2, ai)$	$p(\mathbf{u}_\beta; k = 3, ai)$	$p(\mathbf{u}_\beta; k = 4, ai)$
$-\infty - ai_1$	-	-	-	-
$ai_1 - ai_2$	-	-	-	-
$ai_2 - ai_3$	-	-	-	-
$\dots$	-	-	-	-
$ai_9 - \infty$	-	-	-	-

Table 1: An illustration of the values needed to calibrate acoustic impedance (*ai*), or any other seismic attribute, with the probability (or proportion) of each facies type  $p(\mathbf{u}_\beta; k, ai), k = 1, \dots, K$ .

The calibration procedure consists of determining the seismic-derived prior probabilities  $p(\mathbf{u}_\beta; k, ai), k = 1, \dots, K$  for each *ai* acoustic impedance value. The calibration is accomplished by dividing the range of *AI*-variability into a series of classes, say 10 classes based on the deciles of the *AI* histogram. For each *ai* datum, at a well location, there are corresponding actual proportions of each facies. Combining the facies proportions for all *ai* values within the same class removes the variability that will be encountered from sample to sample. The result of this calibration exercise is a table of prior probabilities. Table 1 shows an empty calibration table for  $K = 4$  facies types and 10 *ai* classes.

Of particular concern in constructing such a calibration table is the vertical resolution of the seismic data. The seismic data (*ai*-values) may be recorded at a small sample rate (2 ms or less); however, the “real” vertical resolution may be much coarser. It is necessary to consider a vertical window of realistic size to calculate the prior probabilities:  $p(\mathbf{u}_\beta; k, ai), k = 1, \dots, K$ . Otherwise, the calibration will not be representative of the true seismic resolution and short scale noise may mask the value of the seismic data.

## Indicator Variogram Inference

Regardless of which variant of indicator simulation is used, we must infer a set of  $K$  indicator variograms that describe the spatial correlation structure of each facies type. The main challenge in variogram inference is the horizontal direction; there are often too few wells to calculate a reliable horizontal variogram. The vertical resolution, however, usually permits a reliable vertical variogram to be calculated. It is difficult to use geological expertise or analogue data for this problem because of the lack of a reliable database. Our approach is to use the seismic data to guide the selection of horizontal parameters for the indicator variograms.

Each facies indicator variogram will be calculated in turn. The first step is to calculate the vertical indicator variogram  $\gamma_k(\mathbf{h})$  from the well data and standardize it to unit sill by the variance  $p_k(1-p_k)$ . Secondly, calculate the horizontal variogram from the corresponding seismic proportions, i.e., the  $p(\mathbf{u}_\beta; k, ai)$  values. The seismic proportion variograms depend on facies type  $k = 1, \dots, K$ ; however, there is unavoidable overlap since the proportions come from the same underlying acoustic rock properties. The seismic  $p_k$  variogram is also standardized to unit sill. Finally, the vertical and horizontal variograms are fit with the shape of the vertical indicator variogram - only the length scales or ranges and any zonal

anisotropy is taken from the seismic proportion variogram.

There are a number of assumptions in this hybrid approach to determine indicator variograms. The most important assumption is that the  $p_k$  variogram provides a reasonable approximation to the horizontal indicator  $i$  range. This is reasonable if the seismic is well correlated to the facies proportions and if the vertical averaging of the seismic is not too pronounced. A second constraint is that we cannot identify zonal anisotropy because we have no consistent 3-D dataset for variogram calculation. This is probably incorrect; however, no other data is available to assist us with inference. Notwithstanding these limiting assumptions, there is little alternative in presence of limited “hard” well data. Of course, experience from other better-drilled reservoirs in the same basin could be used.

An example of the steps in this procedure is presented later with the case study.

## The Bayesian Updating Approach

No further inference is required to apply the *Bayesian Updating Approach* to integrate the seismic data in SIS; the indicator variograms and calibration are sufficient. This method is gaining in popularity because of its simplicity and ease with which seismic is accounted for [7, 8, 9].

At each location along the random path (recall procedure described above), indicator kriging is used to estimate the  $i^*(\mathbf{u}; k), k = 1, \dots, K$  values from hard  $i$  data alone, then the probabilities are modified (updated) as follows:

$$i^{**}(\mathbf{u}; k) = i^*(\mathbf{u}; k) \cdot \frac{p(\mathbf{u}_\beta; k, ai)}{p_k} \cdot C \quad k = 1, \dots, K \quad (3)$$

where  $i^{**}(\mathbf{u}; k)$  are the updated probabilities for simulation,  $p(\mathbf{u}_\beta; k, ai)$  is the seismic-derived probability of facies  $k$  at location  $\mathbf{u}$  being considered,  $p_k$  is the overall proportion of facies  $k$ , and  $C$  is a normalization constant to ensure that the sum of the final probabilities is 1.0. The factor  $p(\mathbf{u}_\beta; k, ai)/p_k$  operates to increase or decrease the probability depending on the difference of the calibrated facies proportion from the global proportion.

The simplicity and utility of this approach is appealing. There are two implicit assumptions behind Bayesian updating that may be important (1) the collocated seismic data perfectly screens nearby seismic data - a Markov type model of coregionalization or cross variability between seismic and facies indicator, and (2) the scale of the seismic is implicitly assumed to be the same as the geological cell size. The block cokriging approach is theoretically more rigorous and can be considered for comparison purposes. The first step in the cokriging process is to infer a licit model of coregionalization.

## Cross/Seismic Variogram Inference

The premise of this paper is that rigorous accounting of the scale and precision of seismic data leads to better reservoir models. As stated above, this calls for a seismic variogram and a cross well-seismic variogram at a small scale. The inference of such variogram models is critical to the proposed method.

Cokriging requires  $i$ ,  $i - p$ , and  $p$  variograms at a small scale for all facies types,  $k = 1, \dots, K$ . At this point we only have the  $i$  variograms that have been defined from both well

data and seismic data. Cokriging requires a positive definite model of coregionalization. In particular, the linear model of coregionalization (LMC) is used almost exclusively in geostatistics [12]. For each facies  $k = 1, \dots, K$  the LMC model would take the form:

$$\begin{aligned}\gamma_{i,i}(\mathbf{h}) &= C_{i,i}^1 + C_{i,i}^2 \cdot \Gamma^2(\mathbf{h}) + C_{i,i}^3 \cdot \Gamma^3(\mathbf{h}) \dots \\ \gamma_{i,p}(\mathbf{h}) &= C_{i,p}^1 + C_{i,p}^2 \cdot \Gamma^2(\mathbf{h}) + C_{i,p}^3 \cdot \Gamma^3(\mathbf{h}) \dots \\ \gamma_{p,p}(\mathbf{h}) &= C_{p,p}^1 + C_{p,p}^2 \cdot \Gamma^2(\mathbf{h}) + C_{p,p}^3 \cdot \Gamma^3(\mathbf{h}) \dots\end{aligned}\tag{4}$$

where  $\Gamma^j, j = 1, \dots, n_s$  are common variogram models of specified type (spherical, exponential, Gaussian, ...), range, and anisotropy. Only the sill  $C$  parameters are allowed to vary between the three variogram models. Moreover the  $C$  values must satisfy the following constraints:

$$\begin{aligned}C_{i,i}^i &> 0 \quad \forall i \\ C_{p,p}^i &> 0 \quad \forall i \\ C_{i,i}^i \cdot C_{p,p}^i &> C_{i,p}^i \cdot C_{i,p}^i \quad \forall i\end{aligned}\tag{5}$$

the underlying hypothesis is that the  $i$  and  $p$  variables are linear combinations of a common pool of random variables.

In the present context we have the basic nested structures from our  $i$  variogram models. The essential step now is to link the large  $V$  scale seismic  $p, p$  variogram and the large  $V$  scale cross  $i, p$  variogram to small  $v$  scale models that can be fit with the linear model of coregionalization described above. For illustration, the basic relations to “downscale” a  $p, p$  variogram will be described below, see also [13, 5]. The same procedure may be applied to the cross variogram.

1. The nugget effect decreases as a variable is averaged to larger scale; the nugget is higher for small scale data. Since the nugget variance is, by definition, random, the scaling relation is as follows:

$$\left[ C_p^0 \right]_v = C_p^0 \cdot \frac{|V|}{|v|}\tag{6}$$

where the  $v$  subscript denotes the geological modeling scale,  $|V|$  is the size of seismic volume, and  $|v|$  is the size of the geological modeling cells.

2. The ranges of the basic structures are reduced by the size of the averaging volume

$$a_v = a_V - (|V| - |v|)\tag{7}$$

where the notation  $|V|$  and  $|v|$  are used here to denote the dimension of the averaging volume in different directions. For example, if  $V$  and  $v$  are the same size in one particular direction (say, horizontally) then the range does not change. Of course, the vertical range would almost certainly be different since the  $V$ -scale is 10-50 times larger than the geological modeling scale.

3. The sill of each basic structure is increased for smaller scales. In this case (as compared to the nugget effect discussed above) we need to account for the specific nature of the variogram. The scaling relationship:

$$\left[ C_p^j \right]_v = C_p^j \cdot \frac{1 - \bar{\Gamma}^j(v, v)}{1 - \bar{\Gamma}^j(V, V)} \quad (8)$$

where the average variogram  $\bar{\Gamma}^j(v, v)$  and  $\bar{\Gamma}^j(V, V)$  values are the classical “gamma-bar” values calculated using the point range.

The variance of the small scale  $p$  values is the sum of the downscaled  $C$  values, that is,

$$\left[ \sigma_p^2 \right]_v = \sum_j \left[ C_p^j \right]_v \quad (9)$$

Where the small scale variance is always greater than the large scale variance; the variance always decreases when a variable is averaged to a larger scale. Note that we can apply these same relations with the cross variogram. The variance in equation 9 would be a cross covariance. These relations can be applied directly to “downscale” the sill parameters of the seismic  $p_k$  variograms. The difficulty is inference of the cross  $i - p$  variogram, since there are too few well data to reliably inform an experimental cross variogram (even in the vertical direction after averaging to the  $V$ -scale). We will make two key assumptions to establish the cross variogram parameters: (1) the sill of the cross variogram is the small scale cross covariance, and (2) the shape of the cross variogram is the same as the shape of the direct  $i, i$  variogram. These are justifiable since the sill of the cross variogram is the cross covariance unless there is zonal anisotropy and the shape of the direct  $i, i$  variogram is certainly related to the cross variogram. Moreover, the LMC requires the same nested variogram structures. Therefore, the cross variogram parameters are given by:

$$C_{i,p}^j = C_i^j \cdot [\rho_{i,p}]_v, \quad j = 0, 1, \dots \quad (10)$$

where  $[\rho_{i,p}]_v$  is the correlation between the small scale indicator data and seismic data. A correlation coefficient has been used rather than a covariance because it is more intuitive to most people (which makes it easier to check the model parameters before using them). As a consequence, the sill parameters for the small scale indicator variogram  $\gamma_{i,i}(\mathbf{h})$  and the small scale seismic variogram  $\gamma_{p,p}(\mathbf{h})$  must be normalized to sum to 1.

The small scale correlation coefficient  $[\rho_{i,p}]_v$  can be determined from the large scale correlation coefficient  $[\rho_{i,p}]_V$ , which can be calculated from the calibration data. That is,  $[\rho_{i,p}]_V$  is calculated by cross plotting the actual proportion of facies at the well locations against the seismic predictions. The downscaling equations given above are used to calculate the small scale correlation coefficient. The procedure can be automated and requires no interpretation, hence it can be left to computer code. The small scale correlation coefficient  $[\rho_{i,p}]_v$  is calculated from the small scale sill / variance values:

$$[\rho_{i,p}]_v = \frac{\left[ \sigma_{i,p}^2 \right]_v}{\sqrt{\left[ \sigma_i^2 \right]_v \left[ \sigma_p^2 \right]_v}} \quad (11)$$

where the variance values are given by:

$$\left[\sigma_i^2\right]_v = \frac{\sum_j^j \left[C_i^j\right]_v \cdot f_j}{\sum_j \left[C_i^j\right]_v} \quad \text{and} \quad \left[\sigma_p^2\right]_v = \frac{\sum_p^j \left[C_p^j\right]_v \cdot f_j}{\sum_j \left[C_p^j\right]_v} \quad (12)$$

note that the  $f_j$  values are the scaling factors in downscaling equations 6 and 8.

Application of this procedure leads to a complete LMC model of coregionalization that can be used for block cokriging with the seismic data and well data. Of course, the model must be checked to ensure positive definiteness (see 5) and adjusted if necessary.

### Block Cokriging

Block cokriging accounts for the scale of the seismic data and the calibration from acoustic impedance to facies proportions. The cokriging formalism is classical; however, most geo-statistical modeling applications consider the different data types to be at the same spatial scale. Once a small scale LMC model of coregionalization has been established, spatial averages of the variogram ( $\bar{\gamma}$  or gamma-bar values) are used in the cokriging equations.

Solution of the cokriging system of equations leads to the weights needed by equation (2), that is, the  $\lambda_\alpha$  and  $\lambda'_\beta$  weights applied to the hard and soft data. We should comment that implementation of block cokriging in a conventional SIS program (such as `sisim` in GSLIB [4]) is straightforward.

## Application to Albacora

The offshore Albacora field consists of deep water turbidite sands, shales, and cemented sands. The important upper portion of the reservoir was modeled with seven vertical wells and two horizontal wells. The model was constructed with constant thickness (2.5 m) cells conforming to the reservoir top. Based on prior geological work, four facies were considered in the sequential indicator simulation: (1) types 1 & 2.1 (clean sandstone with up to about 15% concretions), (2) type 2.2 (up to 30% concretions), (3) type 3 (about one half a combination of concretions and shale), and (4) types 4 & 5 (non-reservoir). The distinction between facies types 2 and 3 is that 3 has a slightly greater amount of non-reservoir rock and it contains shales that have greater lateral continuity than the concretions. The laterally continuous shales of facies type 3 may lead to a reduced vertical permeability.

Figure 1 shows a base map with the seven well locations. A cross section through four wells showing interpreted geologic correlation is shown on Figure 2. The model described here goes from the top of the reservoir to the “B” horizon. The “C” horizon marked on the Figure 2 is largely cemented and is added deterministically after modeling the other facies stochastically.

Acoustic impedance from the wells and seismic has a strong negative correlation with the porosity. The porosity distributions within each of the four facies types described above are quite different; therefore, it will be possible to use the seismic data to constrain the 3-D distribution of facies. The facies were assigned to 2.5 m thick cells. Although the well log data provide greater resolution, 2.5 m cells are suitable because (1) the original facies are defined by observing the concretions, shale, and sand over 1-3 m of core, and

(2) the 0.2 m sampling resolution of the well logs is due to the frequent sampling of the tool responses and is not representative of the true volume measured by the well logs. The acoustic impedance AI is available at an interval of 2 ms. Of course, the resolution is not that good (2 ms is approximately 4 meters). Each AI datum represents a vertical average of 4- 8 ms (considered to be about 15 m for this study). This averaging will be considered in modeling facies through the “block cokriging” approach.

An initial assessment of the value of seismic data is shown on Figure 3, which shows a cross plot of seismic impedance (Y axis) versus the proportion of facies 1 (X axis). The correlation of impedance with the proportions of facies 2, 3, and 4 is not as good (see later).

A horizontal slice through impedance cube is shown on Figure 4. A cross section through impedance cube is shown on Figure 5. These slices show significant areal and vertical variations in impedance that, in turn, constrain proportions of facies. Note the low impedance to the northwest and the high impedance to the south. The vertical variations are quite smooth.

The seismic impedance was calibrated to facies proportions and four arrays of proportions were generated. Figure 6 shows a cross plot of the seismic derived proportion of facies 1 (X axis) versus the actual proportion of facies 1 (Y axis). The correlation coefficient here is 0.61, which is used to establish the linear model of coregionalization described above. The correlation coefficients for the other facies are 0.30, 0.64, and 0.39, respectively for facies 2, 3, and 4.

The vertical indicator variogram for facies 1 is shown on Figure 7. Corresponding horizontal variograms through cube of seismic derived proportions of facies 1 is shown on Figure 8. A 3-D variogram model can be put together from these 3 directional variograms. A short FORTRAN program was written to take the indicator variograms (the variogram was different for each of the facies) and perform the downscaling operations presented above. This program also ensures that the result is positive definite.

The indicator variograms could be used directly (before downscaling) to perform sequential indicator simulation without regard for the seismic data. A horizontal slice and cross section of the sequential indicator simulation model (without using the seismic data) are shown on Figures 9 and reffasimxz. Close examination of the model reveals that the well data and variograms are honored; of course, the trends revealed in the seismic data are not honored.

Adding the seismic data with the Bayesian updating approach leads to models that honor the seismic data (once again the indicator variograms are used directly). A horizontal slice and cross section of the sequential indicator simulation model with the Bayesian updating option are shown on Figures 11 and reffasimbaxz.

The full indicator variogram models can be used to build an indicator simulation model with block cokriging. A horizontal slice and cross section of the sequential indicator simulation model with block cokriging are shown on Figures 13 and reffasimbcxz.

The Bayesian updating and the block cokriging models both honor the seismic and appear similar. There is no question that application of Bayesian updating is similar. It is left to future work to perform a rigorous cross validation study to determine the value of the more complete block cokriging approach.

## Conclusions

Reservoir modeling proceeds sequentially. One reservoir model is built at a time to create a family of multiple equiprobable stochastic reservoir models. Each major reservoir layer bounded by chronostratigraphic surfaces is modeled independently and then combined in a final reservoir model. Within a layer, the distribution of facies types is constructed to honor all available well and seismic data. Finally, within each facies type, porosity and permeability can be modeled.

The rigorous approach of block cokriging has been developed for estimation of the required probabilities for sequential indicator simulation. A case study with the Albacora field illustrates the practical applicability of the method. The key to application of block cokriging is the inference of a licit model of coregionalization between the well-based “hard” indicator data and the seismic-derived “soft” indicator data.

Variogram Inference is difficult in practice because of (1) sparse well data, which makes horizontal variogram inference difficult, and (2) the vertical averaging of the seismic data, which makes it difficult to fit the required model of coregionalization at a small scale. These problems were addressed by a hybrid approach to variogram inference and the use of classical equations for variogram averaging.

A number of assumptions have been documented throughout this paper. One aspect of future work is to consider if these assumptions can be relaxed and to document situations where they are inappropriate. A second aspect of future work is to consider further case studies.

## References

- [1] F. G. Alabert. Stochastic imaging of spatial distributions using hard and soft information. Master’s thesis, Stanford University, Stanford, CA, 1987.
- [2] A. S. D. Almeida. *Joint Simulation of Multiple Variables With A Markov-Type Coregionalization Model*. PhD thesis, Stanford University, Stanford, CA, 1993.
- [3] R. A. Behrens, M. K. MacLeod, and T. T. Tran. Incorporating seismic attribute maps in 3d reservoir models. In *1996 SPE Annual Technical Conference and Exhibition Formation Evaluation and Reservoir Geology*, pages 31–36, Denver, CO, October 1996. Society of Petroleum Engineers. SPE Paper Number 36499.
- [4] C. V. Deutsch and A. G. Journel. *GSLIB: Geostatistical Software Library and User’s Guide*. Oxford University Press, New York, 2nd edition, 1998.
- [5] C. V. Deutsch and H. Kupfersberger. Geostatistical simulation with large-scale soft data. In V. Pawlowsky-Glahn, editor, *Proceedings of IAMG’97*, volume 1, pages 73–87. CIMNE, 1993.
- [6] C. V. Deutsch, S. Srinivasan, and Y. Mo. Geostatistical reservoir modeling accounting for the scale and precision of seismic data. In *1996 SPE Annual Technical Conference and Exhibition Formation Evaluation and Reservoir Geology*, pages 9–19, Denver, CO, October 1996. Society of Petroleum Engineers. SPE Paper Number 36497.

- [7] P. M. Doyen, L. D. den Boer, and W. R. Pillet. Seismic porosity mapping in the ekofisk field using a new form of collocated cokriging. In *1996 SPE Annual Technical Conference and Exhibition Formation Evaluation and Reservoir Geology*, pages 21–30, Denver, CO, October 1996. Society of Petroleum Engineers. SPE Paper Number 36498.
- [8] P. M. Doyen, D. E. Psaila, and L. D. den Boer. Reconciling data at seismic and well log scales in 3-d earth modelling. In *1997 SPE Annual Technical Conference and Exhibition Formation Evaluation and Reservoir Geology*, pages 465–474, San Antonio, TX, October 1997. Society of Petroleum Engineers. SPE Paper # 38698.
- [9] P. M. Doyen, D. E. Psaila, and S. Strandenes. Bayesian sequential indicator simulation of channel sands from 3-d seismic data in the oseberg field, norwegian north sea. In *69th Annual Technical Conference and Exhibition*, pages 197–211, New Orleans, LA, September 1994. Society of Petroleum Engineers. SPE paper # 28382.
- [10] F. Fournier. Integration of 3d seismic data in reservoir stochastic simulations. In *1995 SPE Annual Technical Conference and Exhibition Formation Evaluation and Reservoir Geology*, pages 22–25, Dallas, TX, October 1995. Society of Petroleum Engineers. SPE paper # 30564.
- [11] F. Fournier and J.-F. Derain. A statistical methodology for deriving reservoir properties from seismic data. *Geophysics*, pages 1437–1450, September-October 1995.
- [12] P. Goovaerts. *Geostatistics for Natural Resources Evaluation*. Oxford University Press, New York, 1997.
- [13] A. G. Journel and C. J. Huijbregts. *Mining Geostatistics*. Academic Press, New York, 1978.
- [14] G. Matheron, H. Beucher, H. de Fouquet, A. Galli, D. Guerillot, and C. Ravenne. Conditional simulation of the geometry of fluvio-deltaic reservoirs. SPE paper # 16753, 1987.
- [15] W. Xu, T. T. Tran, R. M. Srivastava, and A. G. Journel. Integrating seismic data in reservoir modeling: the collocated cokriging alternative. In *67th Annual Technical Conference and Exhibition*, pages 833–842, Washington, DC, October 1992. Society of Petroleum Engineers. SPE paper # 24742.

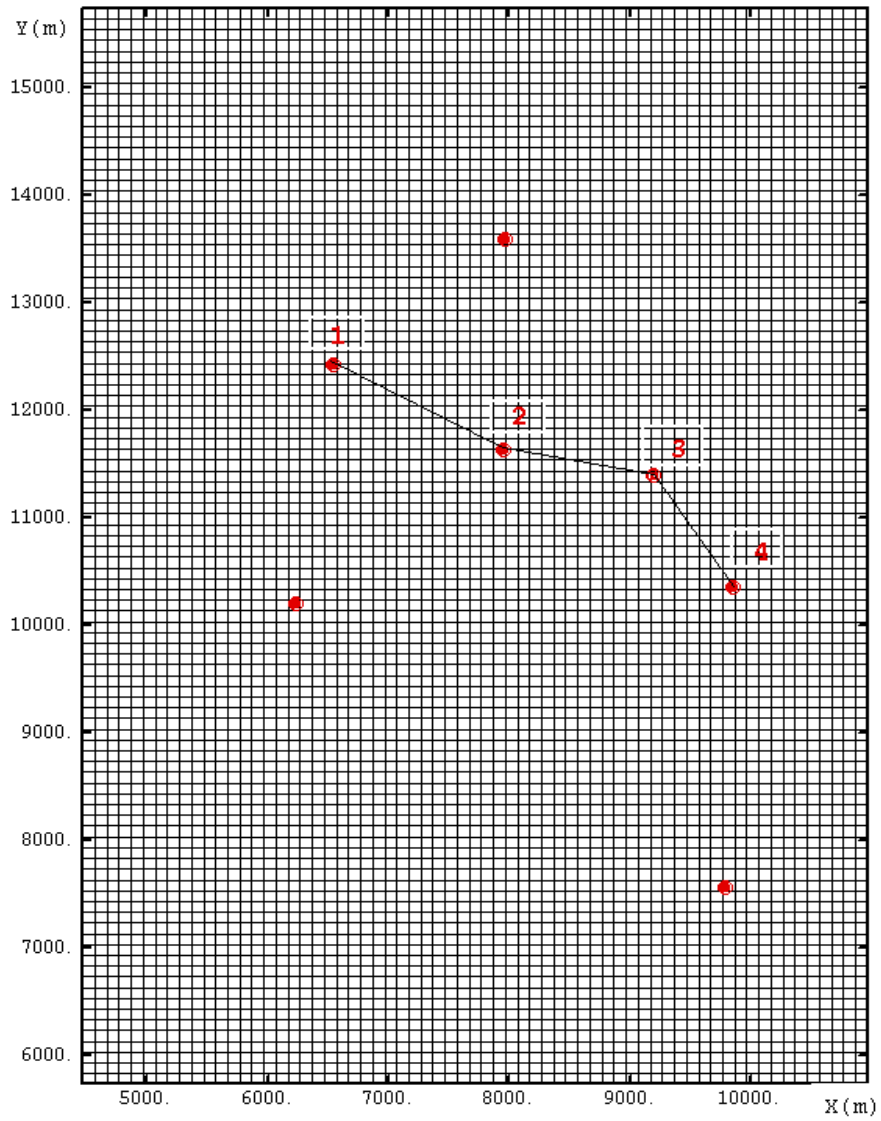


Figure 1: Base map showing the well locations and areal extent of reservoir being modeled.

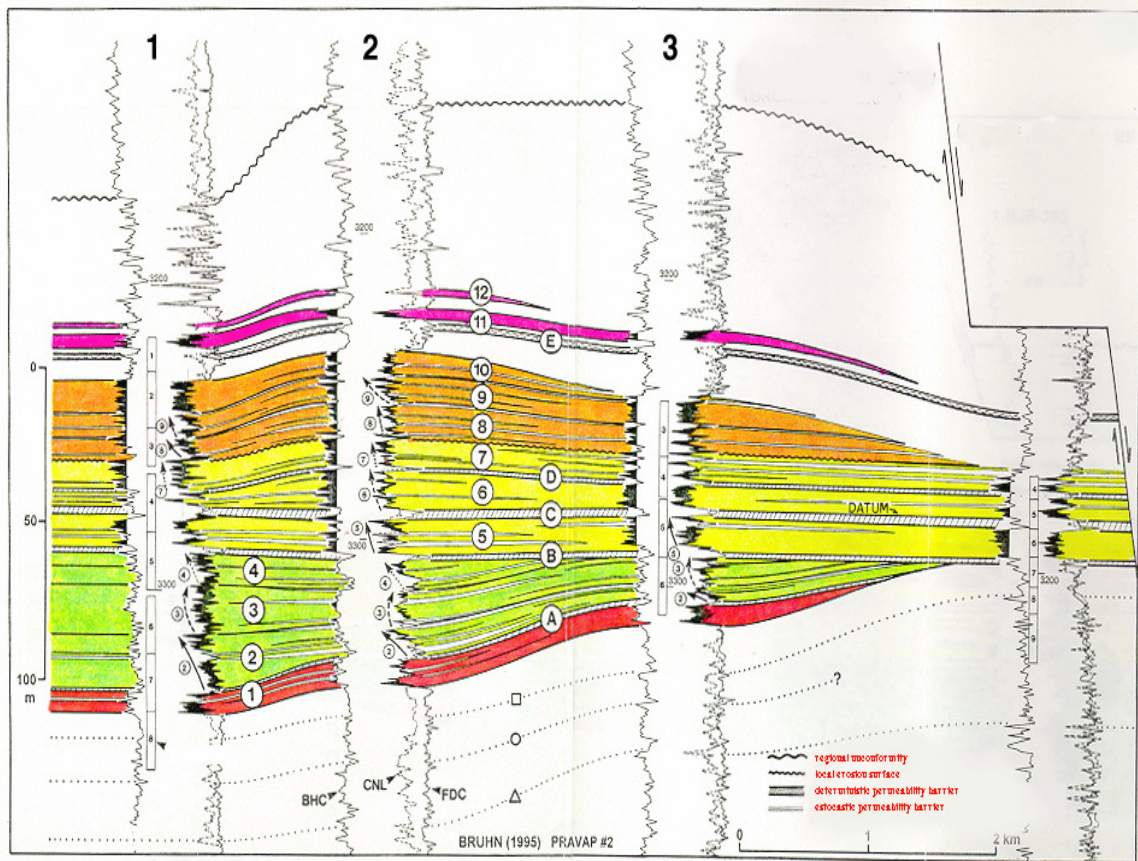


Figure 2: Cross section through three wells showing interpreted geologic correlation.

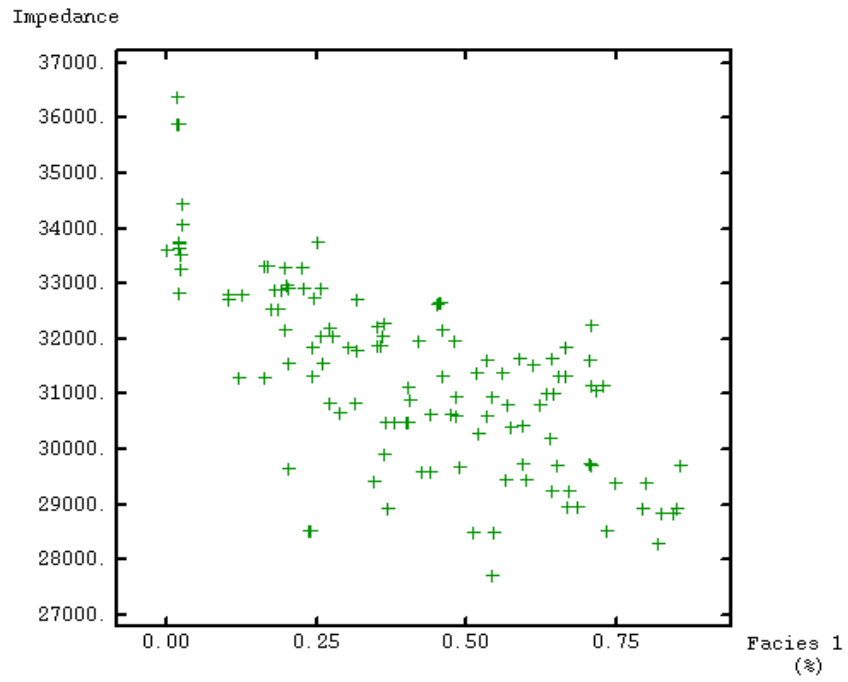


Figure 3: Cross plot of seismic impedance (Y axis) versus the proportion of facies 1 (X axis). Note the good correlation.

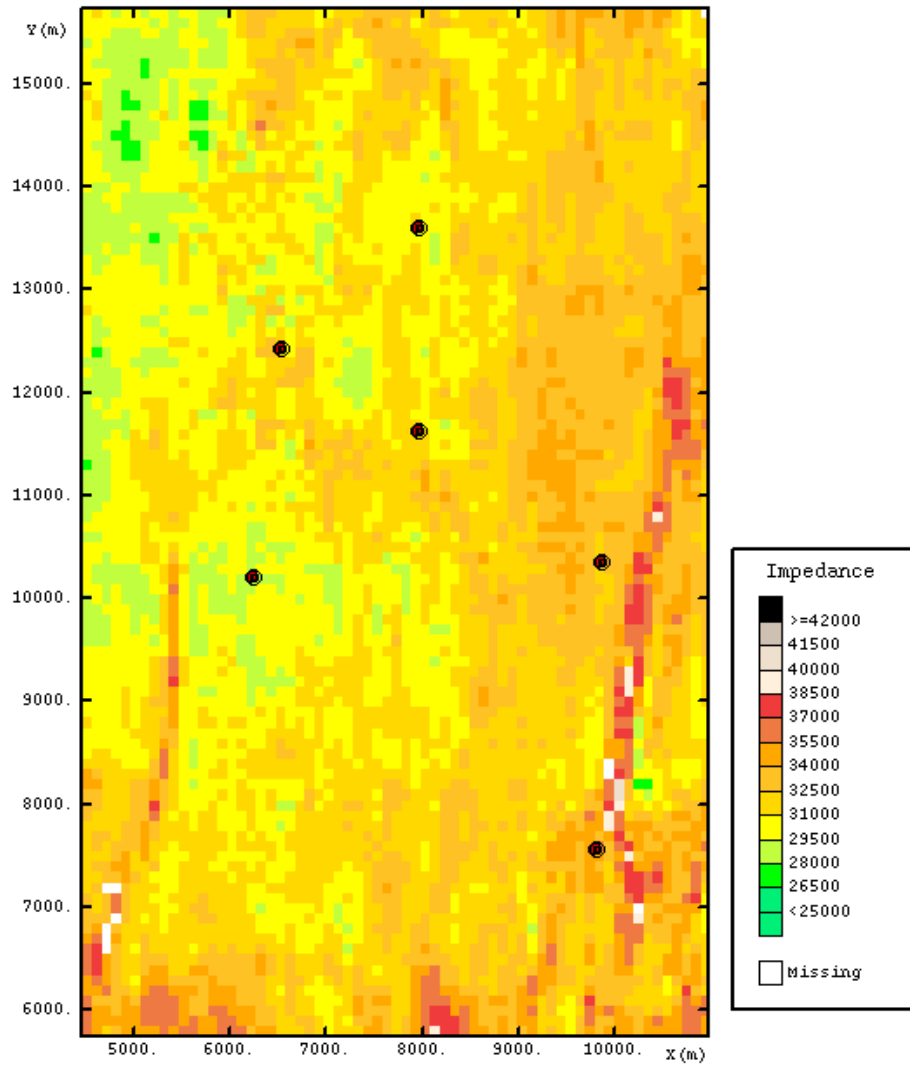


Figure 4: Horizontal slice through impedance cube.

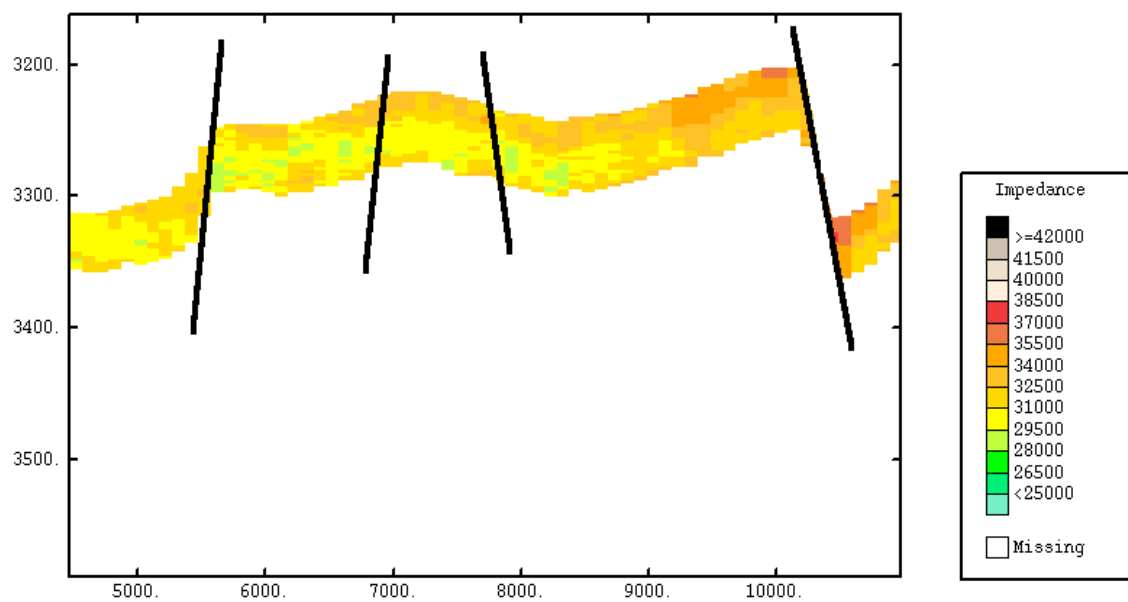


Figure 5: Cross section through impedance cube.

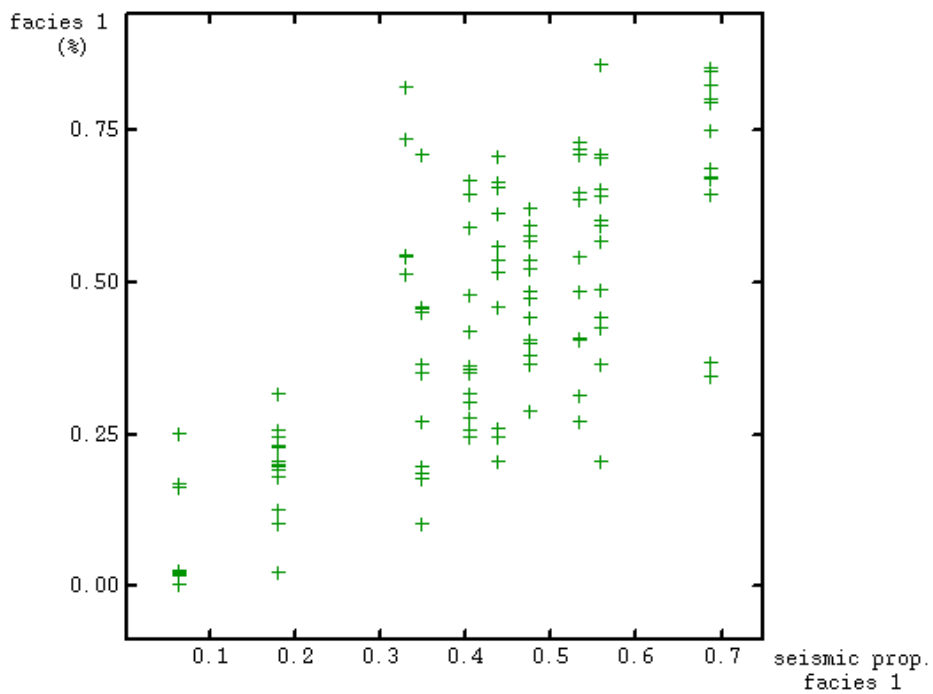


Figure 6: Cross plot of seismic derived proportion (X axis) versus the actual proportion of facies 1 (Y axis).

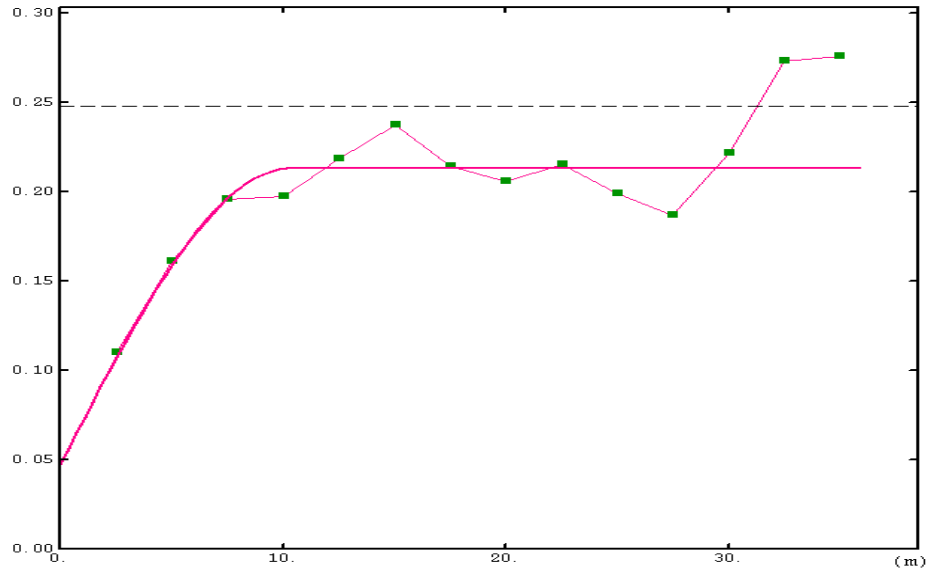


Figure 7: Vertical indicator variogram for facies 1.

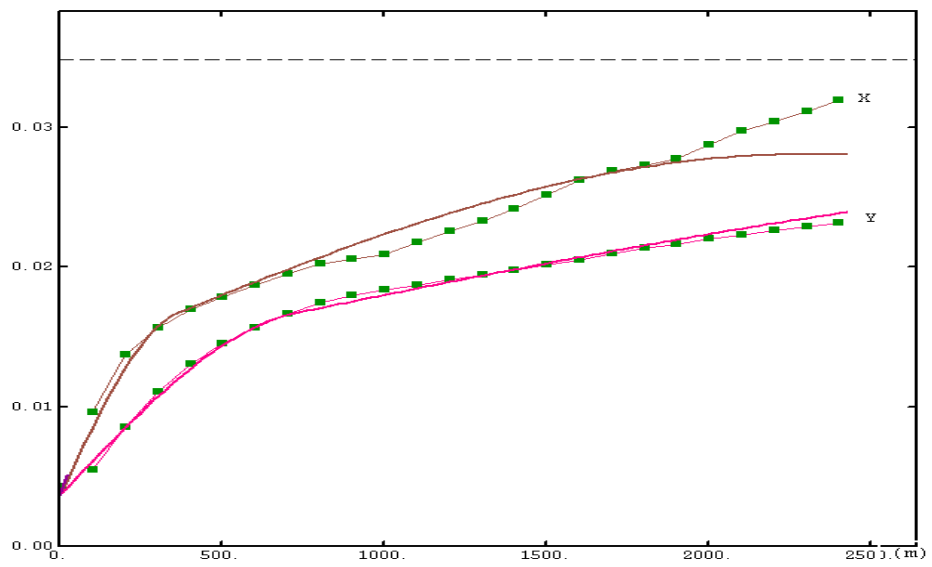
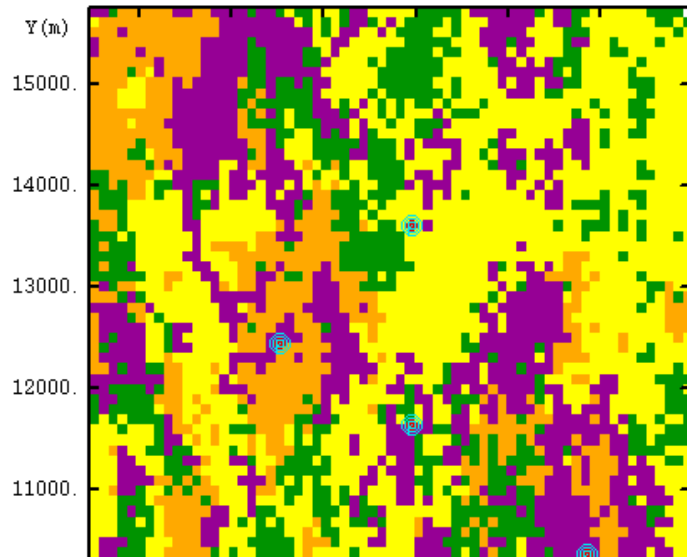


Figure 8: Directional horizontal variograms through cube of seismic derived proportions of facies 1.



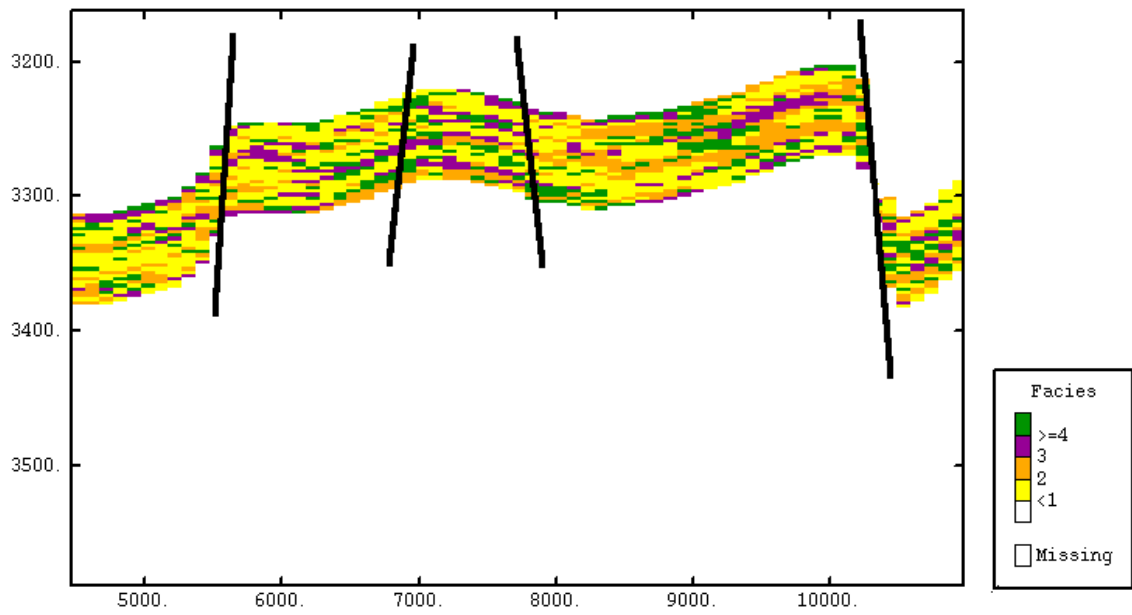


Figure 10: Cross section through facies model generated by sequential indicator simulation (no seismic data).

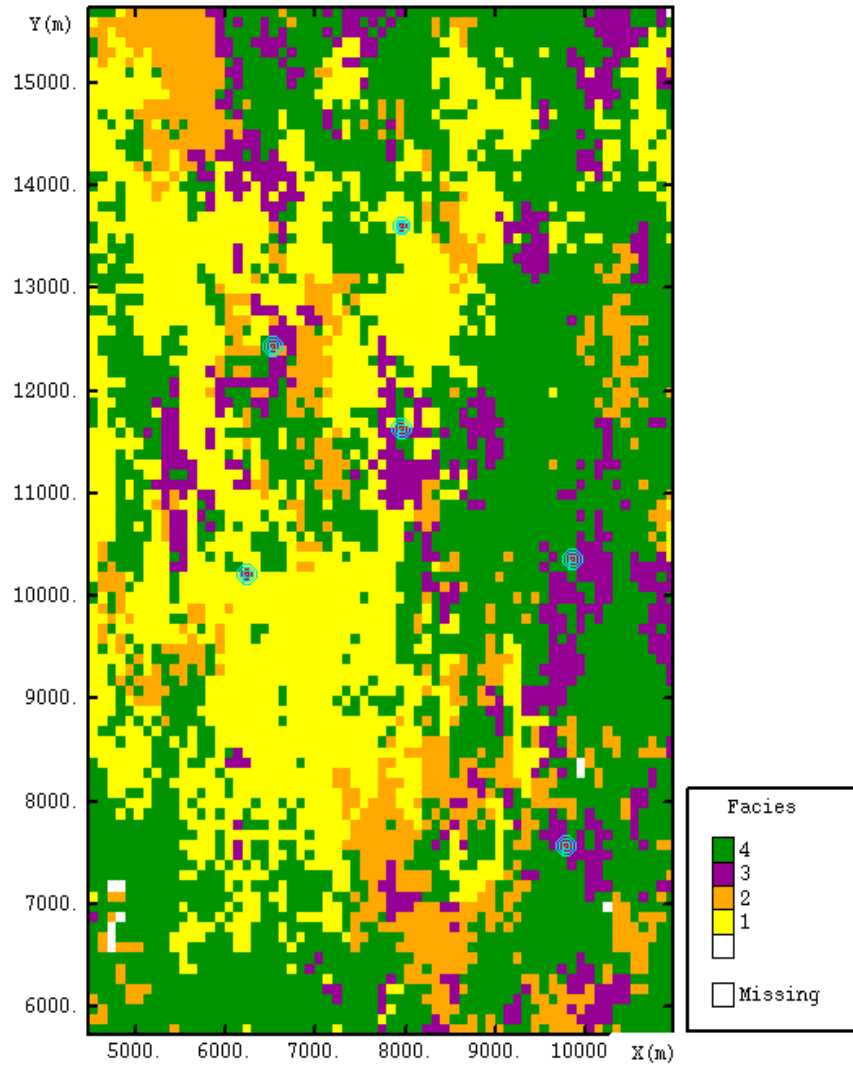


Figure 11: Horizontal slice through facies model generated by sequential indicator simulation with Bayesian updating.

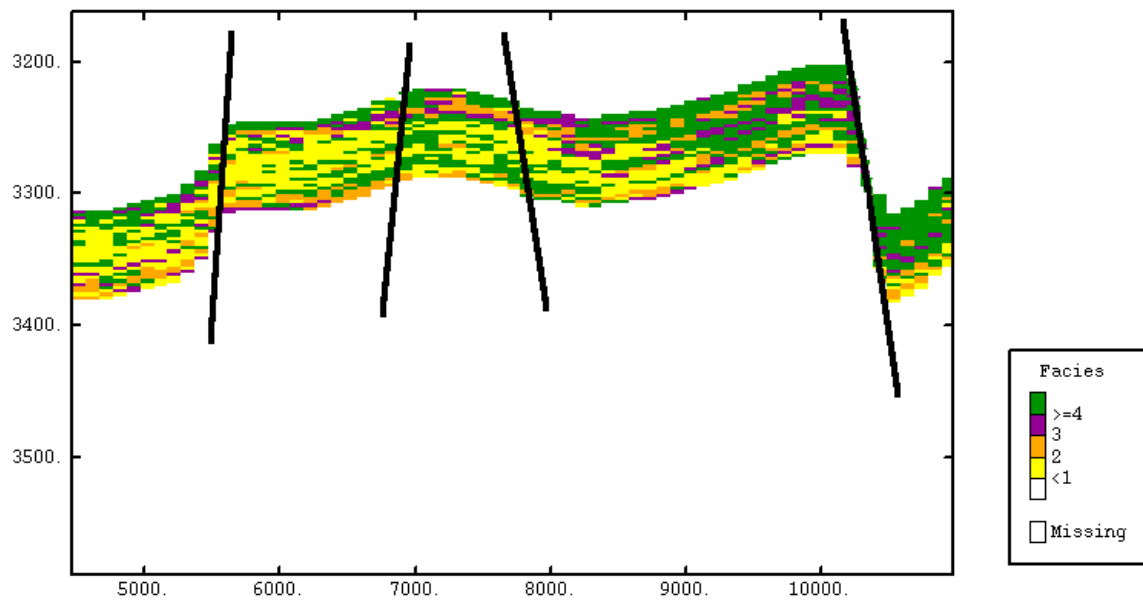


Figure 12: Cross section through facies model generated by sequential indicator simulation with Bayesian updating.

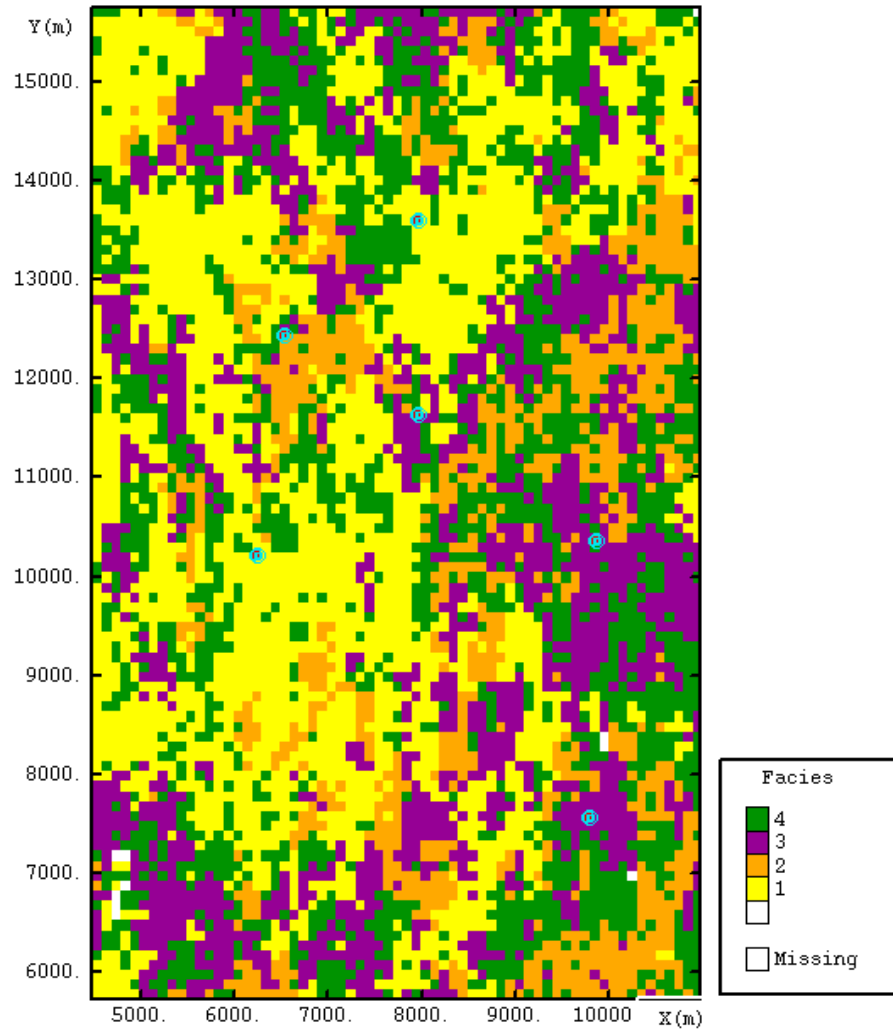


Figure 13: Horizontal slice through facies model generated by sequential indicator simulation with Block cokriging.

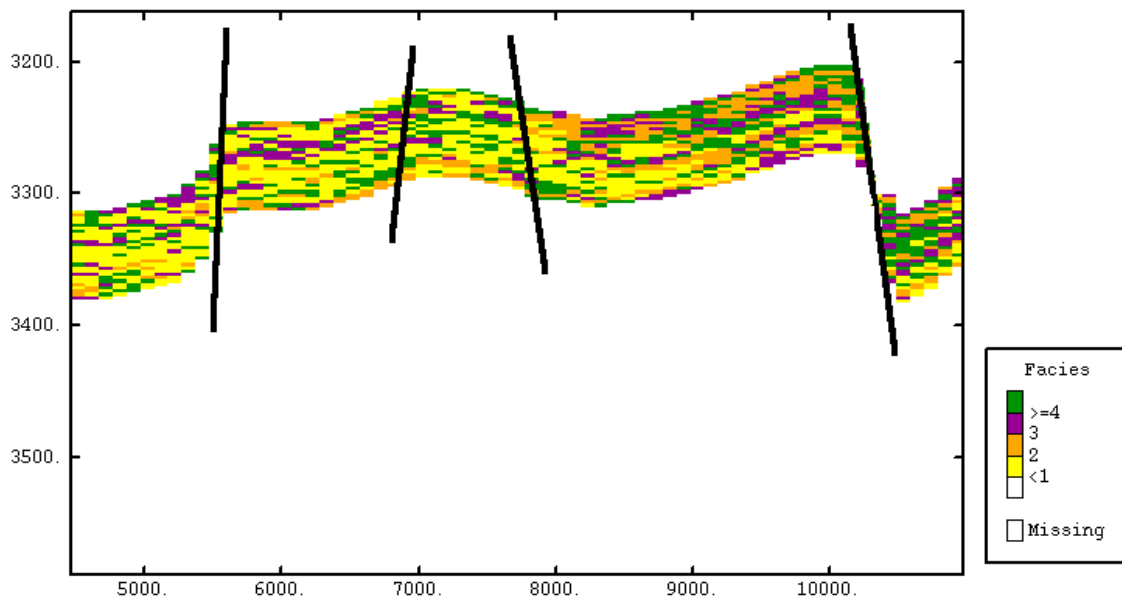


Figure 14: Cross section through facies model generated by sequential indicator simulation with Block cokriging.